International Journal of Disaster Risk Reduction 72 (2022) 102857

Contents lists available at ScienceDirect

International Journal of Disaster Risk Reduction

journal homepage: www.elsevier.com/locate/ijdrr

Remote sensing-based comparative damage assessment of historical storms and hurricanes in Northwestern Florida

Alican Karaer[a,*], Mingyang Chen[b], Michele Gazzea[c], Mahyar Ghorbanzadeh[a], Tarek Abichou[a], Reza Arghandeh[c], Eren Erman Ozguven[a]

[a] *Department of Civil & Environmental Engineering, FAMU & FSU College of Engineering, Resilient Infrastructure and Disaster Response (RIDER) Center, 2035 E Paul Dirac Drive Suite 200 Sliger Building, 32310, Tallahassee, FL, USA*
[b] *Harbin Institute of Technology, Central Research Institute of Building and Construction, Shenzhen, China*
[c] *Department of Computer Science and Electrical Engineering, Western Norway University of Applied Sciences, Bergen, Norway*

A R T I C L E I N F O

Keywords:
Hurricane debris
Catastrophic storms
Resilient transportation systems
Remote sensing
NDVI
Google earth engine

A B S T R A C T

Transportation systems are vulnerable to catastrophic storms while their recovery is vital for returning a community to its pre-storm state. Therefore, performing an accurate damage evaluation and identifying the patterns based on the strengths of these extreme weather events are essential for emergency professionals. A critical problem associated with this damage assessment is the logistics of quickly coordinating and implementing an extensive ground-based damage survey. Another significant challenge in developing a predictive understanding of the long-term effects of storms on coastal communities is the development of quantitative models that can relate the storm intensity and the resulting severity of damage on the different zones of the impacted areas. It is also unclear how urbanization and critical infrastructure affect the extent of the damage caused by them. Thus, this paper introduces a remote sensing-based approach that can rapidly analyze the damage caused by catastrophic storms with different strengths while providing a weighted statistical comparative assessment. We also evaluate an existing debris volume estimation method developed by the U.S. Army Corps of Engineers (USACE) and compare the results to validate the proposed model. Results indicate that suburban and urban areas as well as moderate and high roadway density areas have generated more debris than rural and low roadway density areas. This relationship was also observed based on the normalized difference vegetation index (NDVI) reductions. Findings of this study can help to perform more accurate and faster damage assessments using satellite imagery and remote sensing techniques.

1. Introduction

Catastrophic storms such as hurricanes are among the most lethal and costly natural disasters affecting mankind. In recent years, social and economic damages caused by hurricanes have increased dramatically, which has raised greater concern among the public. While the loss of life can be greatly reduced by a highly successful program of warnings for evacuations and emergency response, property losses and failures on critical infrastructure links are increasing rapidly due to accelerated construction in hurricane-prone areas. This draws attention to the importance of infrastructure performance subjected to hurricanes and assessing the hurricane

* Corresponding author.
E-mail addresses: akaraer@fsu.edu (A. Karaer), adam_2021@qq.com (M. Chen), Michele.Gazzea@hvl.no (M. Gazzea), mg17x@my.fsu.edu (M. Ghorbanzadeh), abichou@eng.famu.fsu.edu (T. Abichou), rajo@hvl.no (R. Arghandeh), eozguven@fsu.edu (E.E. Ozguven).

https://doi.org/10.1016/j.ijdrr.2022.102857
Received 9 October 2021; Received in revised form 14 February 2022; Accepted 15 February 2022
Available online 25 February 2022
2212-4209/

Fig. 1. Study area and selected hurricane/storm tracks.

damages properly. This kind of resilience assessment requires a deeper understanding of the impact of severe storms and hurricanes on communities and infrastructure.

The aftermath of a hurricane often includes a large amount of debris due to infrastructure or landscape damage. Multiple studies have spatially and statistically investigated the impact and damage of hurricanes. For instance, to better understand hurricane damage on residential buildings, Friedland [1] proposed a forecast model to describe and assess residential building damage from a hurricane storm surge. Unlike traditional methods, he categorized hurricane damages on a loss-consistent basis, regardless of the primary intensity mechanism. In a similar study conducted by Massarra [2], a comprehensive building damage assessment was performed including the combination of hurricane winds and flood loads. A protocol to standardize data collection and damage assessment was also suggested so that the performance of multiple buildings can be addressed given various levels of a hazard. Contrary to the detailed assessment, rapid damage assessment was also used to capture a general impression of damaged structures.

Roadway networks have been known to be one of the highly vulnerable infrastructure systems to hurricanes [3–7]. Therefore, it is crucial to better evaluate the roadway infrastructure against hurricanes. Houser [8] focused on the roadways along Santa Rosa Island in Northwest Florida. Their findings indicated that sections of the roadway that experienced major damage or were completely destroyed tended to be in narrow sections of the island where the elevation was relatively high. Ghorbanzadeh et al. [9] have studied the power outages and roadway closures in the City of Tallahassee based on actual data on the impact of Hurricane Hermine (2016) and Michael (2018) throughout the city. Conducting statistical and spatial analyses, this study showed those locations that were under high risk of electricity outages and roadway disruptions.

Remote sensing technologies have been increasingly used for damage assessment purposes [3,7,10,11,40,41]. There are different types of remote sensing data that are useful for post-disaster damage assessment including the following: aerial photo, drone imagery, satellite imagery, and light detection and ranging (LIDAR) data. Jiang and Friedland [12] proposed a methodology for automatic urban debris zone extraction from high-resolution aerial imagery. To separate urban debris from non-debris areas, three classification approaches were used in this paper: spectral, textural, and combined spectral textural methods. The results indicated that multivariate texture information significantly improves debris classification performance by decreasing the confusion between debris and other land cover types. Wang et al. [13] developed a rapid assessment algorithm for post-hurricane forest damage estimation using moderate spatial resolution satellite imagery, which investigated and evaluated the performance of five commonly used vegetation indices. The paper suggested the use of an index, namely the Normalized Difference Infrared Index (NDII), which was identified as the optimal damage indicator among these. Similarly, in a recently published study [3], the authors proposed a data fusion framework combining multispectral satellite imagery and various vector data by comparing the performance of five different vegetation indices to find the most suitable one for post-hurricane debris assessment purposes. Results indicated that Modified Soil Adjusted Vegetation Index (MSAVI2) is slightly better than Normalized Difference Vegetation Index (NDVI) representing the variation in hurricane-caused vegetative debris and both are recommended in lieu of the field data collection.

There are few methods in existence for accurately estimating urban debris in costly natural disasters. The U.S. Army Corps of Engineers (USACE) Emergency Management staff has developed a modeling methodology designed to forecast potential amounts of hurricane generated debris [14]. The model is based on several factors such as hurricane intensity, population, vegetation, and commercial density. The estimated quantities produced by the model have a predicted error of around 30% [15].

A critical problem associated with damage assessment of hurricanes is the logistics of quickly coordinating and implementing an extensive ground-based damage survey. Another significant challenge on developing a predictive understanding of the long-term effects of hurricanes on coastal communities is the development of quantitative models to explain the relationships between the storm intensity and the resulting severity of damage on the different zones of the impacted areas. Moreover, it is unclear that how urbanization and critical infrastructure may affect the extent of the damage caused by hurricanes. As such, the objectives of this paper are to:

- introduce a remote sensing-based approach that can rapidly analyze the damage caused by tropical storms and hurricanes with different strength levels
- provide a statistical comparative method that includes diverse demographic factors to estimate the differences between damages caused by these extreme weather events.
- evaluate an existing debris estimation method developed by the USACE (*14*) and compare their results to validate the proposed model.

2. Study area and selected disasters

2.1. Study site

Among the hurricane-prone areas in the U.S., Bay County of Florida has suffered substantial damages from storms and hurricanes, which led to a catastrophic death toll and property losses. According to the National Oceanic and Atmospheric Administration (NOAA), the Bay County area has experienced a total of 26 hurricanes and tropical storms since 1842 [16]. The county's largest city is Panama City, best known for its white sand beaches and emerald, green water. According to the U.S. Census Bureau, the county has a total area of 1033 square miles, of which 758 square miles is land and 275 square miles is water. As of 2019, the population was estimated to be 174,705 [17]. Fig. 1 highlights the location of Bay County in the State of Florida along with the selected hurricane tracks.

2.2. Overview of selected storms and hurricanes

In this paper, two tropical storms and three hurricanes that impacted Bay County are chosen based on their intensity, direction, and data accessibility. Their names as well as their years and intensities are listed as follows:

1. Tropical Storm Beryl (1994) was one of the reasons that made the 1994 hurricane season so peculiar. It started as a tropical depression and intensified into a tropical storm with maximum sustained winds of 60 mph (95 km/h) before making landfall near Panama City, Florida. Total damage from Beryl was estimated as $73,000,000 [18]. Although Beryl caused no direct fatalities, there were a large number of people injured and harmed by.
2. Tropical Storm Fay (2008) was a strong and unusual tropical storm that moved erratically across the State of Florida and the Caribbean Sea. Unlike other hurricanes, Fay gained strength over Florida's inland waters after the process of weakening due to the landfall. Thirteen deaths were blamed directly to Fay [19]. Damage was primarily caused by rainfall-induced floods that affected residential structures. The total damage of Fay in the U.S. was estimated at about $560 million (*19*).
3. Hurricane Earl (1998) was a short-lived Category 2 hurricane that caused moderate damage throughout the Southeast U.S. It was formed on August 31, 1998 and dissipated on September 8, 1998. Hurricane Earl killed three people and caused $79 million in damage in 1998. Coastal communities were inundated due to severe storm surge and heavy rain induced by the hurricane. The most extensive damage occurred in Bay County where 1112 structures were damaged by flooding and three were destroyed [20].
4. Hurricane Kate (1985) was the final in a series of tropical cyclones to impact the U.S. in 1985. It was formed on November 15, 1985 and disappeared on November 23, 1985. Kate caused destructive storm surge and flooding that crashed coastal infrastructure, which caused many people to lose their jobs in the weeks after the storm. High-speed wind contributed to downed trees and building damage, and downed power poles, leading to extensive power outages. Overall, Kate resulted in 15 fatalities and $700 million in damage [21].
5. Hurricane Michael (2018) is the most intense and recent hurricane in this study. With maximum sustained wind speeds of 161 mph (259 km/h), Hurricane Michael made its landfall near Mexico Beach in the Florida Panhandle region on October 10, 2018. This indicates that it was a Category 5 hurricane based on the Saffir-Simpson Hurricane Wind Scale. Therefore, it became one of the four Category 5 hurricanes on record to have hit the U.S. mainland. It pushed a massive and destructive storm surge to the coast, which resulted in catastrophic damages [22].

Each of these events had its own intensity, which was significantly affected by the maximum wind speed associated with the event. Table 1 presents maximum wind speeds relative to each hurricane and storm. Fig. 1 illustrates the track (path) of each storm and hurricane while passing over the Bay County. The tracking data were obtained from ESRI's Living Atlas [23] and visualized in ArcGIS Pro v2.9. All hurricanes were moving from Southwest (SW) to Northeast (NE) except Tropical Storm Fay, which was traveling from Southeast (SE) to Northwest (NW).

2.3. *The Saffir-Simpson Hurricane Wind Scale*

Wind speeds have often been used to determine the intensity of hurricanes. However, hurricane damage not only comes from the winds, but can also come from rain, tornadoes, floods, and very low air pressure. In the 1970s, a system was developed to characterize the destructive potential of hurricanes and named as the Saffir-Simpson scale after its inventor. In addition to maximum sustained wind speed, the Saffir-Simpson scale considers different levels of central pressure and storm-surge height [24]. The scale is listed in Table 1. Saffir-Simpson Hurricane wind scale includes a 1 to 5 rating based on a hurricane's sustained wind speed. Storms that have maximum sustained surface winds less than 73 mph have been considered as tropical storms. This scale only estimates the potential hurricane damage. Hurricanes reaching Category 3 and higher are considered major hurricanes because of their potential for significant loss of life and damage. However, Category 1 and 2 hurricanes and tropical storms are still dangerous and require preventative measures.

3. Methodology

The methodology adopted in this paper consists of three modules (1): A damage assessment of the aforementioned disasters using the NDVI derived from satellite imagery (2), implementation of the USACE hurricane-caused debris volume estimating model, and (3) a comparative analysis performed between these two methods. Fig. 2 illustrates the process of hurricane damage assessment and comparison. The steps of the methodology are discussed in more detail in the following sections.

Table 1
Saffir-Simpson hurricane scale and associated strengths of selected storms and hurricanes.

Saffir-Simpson Scale (Category)	Central Pressure (inch)	Wind Speeds (mph)	Storm Surge (feet)	Observed Damage
1	≥28.94	74–95	4–5	Minimal
2	28.50–28.91	96–110	6–8	Moderate
3	27.91–28.47	111–130	9–12	Extensive
4	27.17–27.88	131–155	13–18	Extreme
5	<27.17	>155	>18	Catastrophic

Selected Storms and Hurricanes

	Beryl	*Fay*	*Earl*	*Kate*	*Michael*
Year	1994	2008	1998	1985	2018
Max Wind Speed (mph)	60	68	100	120	160
Category	*Tropical Storm*	*Tropical Storm*	*Category 2*	*Category 3*	*Category 5*

3.1. Damage evaluation using NDVI reduction

Although the hurricanes and storms studied in this paper span more than 30 years of a time frame, we have used the Google Earth Engine (GEE) to acquire a single band NDVI for the before and after of each hurricane and storm from the following sensors:

- Landsat 5 (1984–2013) for Hurricane Kate (1985), Tropical Storm Beryl (1994), and Hurricane Earl (1998)
- Landsat 7 (1999–2021) for Tropical Storm Fay (2008)
- Landsat 8 (2013 –) for Hurricane Michael (2018).

Please note that, even though the overall product quality has significantly improved on each new Landsat mission, the moderate spatial resolution (30 m/pixel, ~98.43 feet/pixel) to calculate the NDVI has been maintained since Landsat 4 (1982–1993) [25]. In addition, GEE is a globally recognized platform to acquire, visualize, and process several types of satellite imagery. The platform not only allows user to write codes for customizing the remotely sensed data but it also provides ready to use scripts especially for automated NDVI extraction [26], which was partially employed in this study. To obtain images with a minimum cloud influence on the Bay County area we also used cloud and cloud-shadow masking algorithm Fmask, developed by Zhu et al. [27], which helped to remove images where the cloud cover was greater than 10%. Then, composite images were constructed from an image collection recorded in the 90-day period before and after each hurricane and storm made their landfalls. Finally, the single band NDVI images were calculated from each composite image collection. Because the NDVI data are more accessible and easier to preprocess for the long study period via GEE, it was used in the study as the primary spectral index despite MSAVI2 was found to be slightly more accurate than NDVI to represent the variations on hurricane-caused vegetative debris in our previous study (*3*).

NDVI is proven to be one of the great approaches to analyze the hurricane damage [3,7,10,28]. Particularly, when vegetation was ripped out by the hurricane, trees would fall, plants would die and the chlorophyll would greatly decrease, leading to decrease in NDVI values. Therefore, NDVI values were calculated for each composite image using Equation (1):

$$\mathrm{NDVI} = \frac{\mathrm{NIR} - \mathrm{RED}}{\mathrm{NIR} + \mathrm{RED}} \tag{1}$$

The change of NDVI was obtained by subtracting the NDVI values of before and after storm composite images at the pixel level. The resulting image was converted and exported as a GeoTIFF image for the future analysis and visualization in ArcGIS Pro v2.9 along with the vector data acquired from U.S. Census Bureau for the county borders and population [29] as well as for the street centerlines [30].

Population data were presented by census block groups in polygon type covering the entire county. Roadway data were imported as line features and bounded with block groups. The length of roadways in each population block group was first summed up using the summarize within tool in the utilized GIS software. Then, the population and the total roadway length of each block group were converted to point data at the centroid of each block group. Lastly, the density distribution of the magnitude of population and roadway length were determined using a kernel density estimation (KDE) approach based on the point data at the centroids. Please note that, KDE tool has allowed us to convert the vector data (i.e., population and roadway densities) to raster data with higher pixel values on high population and roadway density areas.

To integrate these preprocessed data, namely the change of NDVI, population density, and roadway density, the Rasterio package, offered in Python programing language by MapBox [31], was used. This package particularly reads and writes those raster datasets while allowing the users to customize and analyze. In order to normalize the input data, a new field was created to scale the magnitude in each dataset from 1 to 10, as a similar approach was adapted in a previous study [42]. For population, this normalized value was divided into three equal intervals as [1,4), [4,7), and [7,10] to label the data as "rural", "suburban", and "urban", respectively as a similar method was used in a previous study [43]. Similarly, for roadway density, the equal intervals of the normalized value were

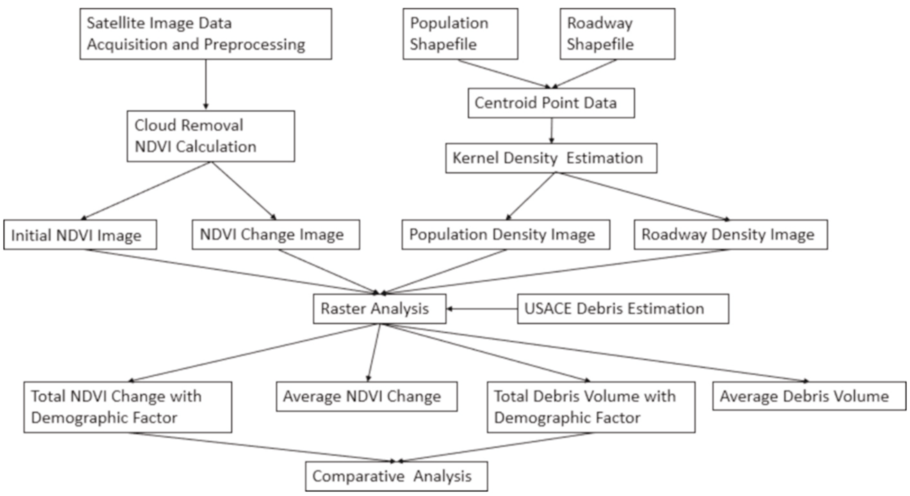

Fig. 2. Flowchart of the proposed methodology.

labeled as “low roadway density”, “moderate roadway density”, and “high roadway density”. Finally, for the NDVI Reduction data the normalized values were labeled as “minor damage”, “moderate damage” and “severe damage”. These were simply a measure of urbanization and hurricane-caused damage at a given block group which helped conceptualize the comparison of the damage caused by different hurricanes and storms in different urbanization settings.

The total NDVI reduction for each storm and hurricane was calculated by summing up each pixel in the block group. Every pixel of NDVI reduction was then analyzed within the aforementioned categories of population and roadway density, separately. Therefore, NDVI reduction under each scenario and average NDVI reduction per pixel were determined.

3.2. USACE debris estimation model

In terms of hurricane damage assessment, the debris data is more difficult to collect than the infrastructure disruption data such as roadway closures and power outages. This makes it harder to evaluate the damage of a hurricane in the context of debris. This issue is mainly because it is difficult to quantify the debris damage. The USACE developed the first debris estimation model using data collected from Hurricanes Frederic (1979), Hugo (1989), and Andrew (1992) (*32*). This model is described in Equation (2):

$$Q = H(C)(V)(B)(S) \tag{2}$$

Q : *Debris Volume* (*cubic yard (cy* $= \sim$*0.76 m*^{3}*))*
V : *Vegegation characteristics multiplier* $= \{1.1,\ 1.3,\ 1.5\}$ for vegetation cover {Light, Medium, Heavy}
B : *Commercial land use multiplier* $= \{1.0,\ 1.2,\ 1.3\}$ for commercial category {Light, Medium, Heavy}
S : *Precipitation multiplier* $= \{1.0,\ 1.3\}$ for precipitation characteristics {None/Light, Medium/Heavy}

Although this was an empirical model, it had the ability to estimate the debris volume with a maximum of ±30% error [32,33]. The first deterministic storm-related debris volume estimation model was developed using the Federal Emergency Management Agency (FEMA) Project Worksheets, based on the support provided for the damage after any of the seven hurricanes during the 2004 and 2005 hurricane season in the State of Florida [34]. 680 Project Worksheets were collected with the expense and debris volume details. The final model calculated the debris volume as 0.77 cubic yard (cy = $\sim$0.765 m^3 = $\sim$27 ft^3) for low damage storms, 4.44 cy for moderate-damage storms, and 22.85 cy for high-damage storms for every 100 ft street segment [35]. Following this concept and using the same dataset, an average of 488 cy vegetative debris with a cost of $21.5 was calculated [36]. Another study focused on the urban forest debris after Hurricane Ike (2008) using permanent plots in Houston, TX (33). The findings revealed that vegetation related variables explained greater variation in tree debris volume than the storm-related meteorological variables such as wind speed. Furthermore, Duryea et al. [37,38] collected tree damage data from the field shortly after the Hurricane Ivan (2005) to evaluate the resilience of single trees by their species, which is very dangerous given the hurricane aftermath conditions. These pioneering studies provided a great knowledge on hurricane vegetative debris generation; however, the major concern was using field data measurements such as tree counts, diameters, and heights for the vegetation cover inputs. These data sets might not be available in certain areas. Collection of such a tree database could be very expensive and intrusive as periodic updates are necessary to evaluate hurricane impacts. A satellite image taken before and after the hurricane can provide sufficient information about vegetation cover that could be used in the damage assessment. Therefore, there is a great potential for using remote sensing data to improve the performance of traditional hurricane damage assessment methods.

To compare the remote sensing-based damage assessment with the USACE’s debris volume estimation, the storm category multiplier was determined based on the intensity of each of the selected storms and hurricanes that hit Bay County. Note that Tropical Storms Beryl and Fay are treated as Category 1 hurricanes since their wind speeds were very close to that of a Category 1 hurricane (Table 1), therefore a value of 2 cy was used as the “C” multiplier for both storms. The assumption of 3 persons per household (H) was used for this model. Therefore, the developed population per pixel values obtained in the population image, which was generated using a KDE approach, was used to determine a value for H as one-third of the population. The determination of vegetation multiplier (V) relayed on initial NDVI value per pixel, which was simply the value before the storm or hurricane hit. The initial NDVI value was also divided into three equal intervals from 0 to 1 and the associated vegetation multiplier is determined. Commercial factor (B) is the multiplier that considers areas that are not solely single-family residential, but it also includes small retail stores, schools, apartments, shopping centers, and light industrial/manufacturing facilities. Considering the development and economy of the Bay County area, the value of 1.1 was selected for this factor. Precipitation multiplier (S) also depends on the hurricane intensity. Hurricanes that were category 3 or greater were considered to have a heavy precipitation with a multiplier of 1.3, while other low-intensity hurricanes belonged to the group with a light precipitation having a multiplier of 1.0. Once all factors were determined, the total volume of debris and average debris per pixel were calculated. In addition, demographic factors of population density and roadway density were used for weighted debris damage evaluation. In this way, debris volume under each scenario could be estimated.

Table 2
Descriptive statistics of NDVI reduction in Bay County, FL.

	Beryl	Fay	Earl	Kate	Michael
Category	Tropical Storm	Tropical Storm	1	3	5
Number of pixels	2,574,805	2,574,765	2,547,831	2,467,861	2,574,656
Mean	0.015	0.011	0.013	0.094	0.113
Standard Deviation	0.042	0.039	0.035	0.065	0.100
Min	0	0	0	0	0
Max	0.586	0.699	0.639	0.701	1.157

4. Results and discussion

4.1. Damage assessment with NDVI reduction

First, descriptive statistics of NDVI reductions in Bay County due to each storm and hurricane are demonstrated in Table 2. Note that the number of pixels was different for each event since the cloud part in each image was removed. The maximum NDVI reduction value was for Hurricane Michael among all the storms, which was 1.157. Hurricanes Kate and Michael had similar mean reduction values around 0.1 while other means for other hurricanes were around 0.013. Hurricane Michael also had the largest standard deviation of 0.1 whereas Hurricane Earl had the smallest standard deviation of 0.035.

NDVI reduction method can highlight the impact only after a certain threshold on the strengths of the storms and hurricanes. For example, Category 3 and Category 5 hurricanes indicate much larger expected NDVI reductions compared to the tropical storms and the Category 1 hurricane. Also, the NDVI reduction exponentially increases after this threshold as the mean reduction increases by 20% from the Category 3 hurricane to the Category 5 hurricane. Based on this observation, total NDVI reductions were analyzed with the given wind speed in mph as a continuous variable instead of a categorical scale while considering the population and roadway density.

The total NDVI reduction of all hurricanes are illustrated in Fig. 3a and Fig. 3b with a focus on the population and roadway density. Note that these storms and hurricanes have their own intensities as assigned by the maximum wind speeds (Table 1). Overall, the reduction of NDVI was low and stable when the intensity of the event was low based on the wind speeds below 100 mph. That is, there is no significant change observed. It is also clear that the total NDVI reduction increased drastically when the intensity reached a peak value based on the maximum wind speed of 120 mph, where the total NDVI reduction increased by a factor of 7.01. The sharp increase in NDVI reduction flattened to a factor less than 1.5 when the hurricane the maximum wind speed increased from 120 mph to 160 knots.

The pattern in rural areas is similar to the overall assessment whereas suburban and urban areas tend to experience more NDVI reduction. When the hurricane intensity increased with a speed reaching 120 mph, the total NDVI reduction increased by a factor of 9.86 for suburban areas and by a factor of 9.36 for urban areas, respectively. Total NDVI reduction based on the roadway density was almost identical, except the total NDVI reduction, a factor of 9.51 for moderate roadway density areas and 9.33 for high roadway density areas once the intensity of the hurricane exceeded 120 mph.

The results of damage assessment for all storms and hurricanes are illustrated in Fig. 4 and Fig. 5 in terms of population and roadway density, respectively. As aforementioned, the extent of damage was classified as "Minor", "Moderate", and "Severe" based on the NDVI reduction caused by storms and hurricanes. Each assessment was weighted with demographic factors of population and roadway density. Overall, Figs. 4 and 5 indicate that Tropical Storm Beryl caused minor damage at approximately 70% of the total area. Tropical Storm Fay and Hurricane Earl also caused minor damage at more than 60% of the total area. Only 20% and 25% of the county experienced minor damage during Hurricane Kate and Michael, respectively.

Figs. 4 and 5 suggest that Hurricane Kate caused the most moderate damage in the county compared to all other hurricanes and storms, and with Hurricane Michael, 45% of the area had moderate damage. On the other hand, Tropical Storm Beryl, Tropical Storm Fay, and Hurricane Earl led to a moderate damage for less than 40% of the area. More importantly, Figs. 4 and 5 reveal that Hurricane Michael was responsible for the most damage where 23% of the area suffered severely. Other hurricanes only caused severe damage for less than 8% of the study area.

Using the population density classification, Fig. 4 suggests that Tropical Storm Beryl, Tropical Storm Fay, and Hurricane Earl produced mainly minor damage in suburban and urban areas. Hurricanes Kate and Michael, on the contrary, caused the most severe damage in suburban and urban areas. Note that the largest portion of severe damage was caused by Hurricane Michael in 35% of the urban areas. This is a critical finding that indicates the difference in how severe hurricanes hit urban areas compared to rural areas. In urban areas, 30–35% of the total area severely impacted after strong hurricanes whereas this rate is 20% in the rural areas experienced severe impacts. Despite the rural areas better represents the overall results, there are more people to be affected in urban and sub urban areas.

Fig. 5 shows that damage assessment based on the roadway density happens to have a similar pattern compared to the case of

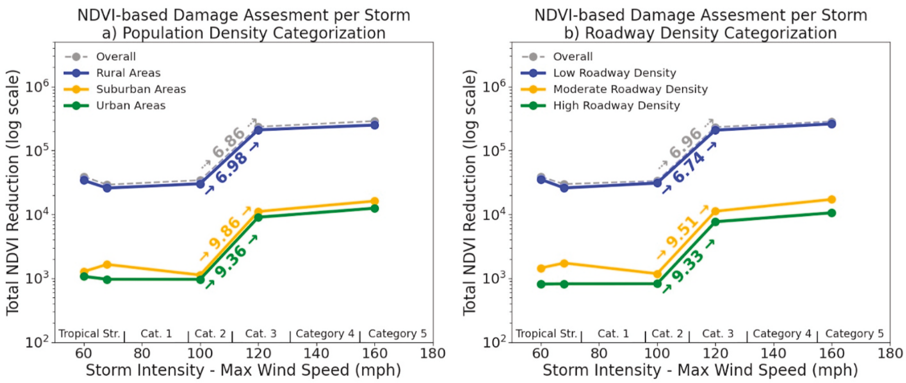

Fig. 3. Total NDVI reduction weighted on (a) population and (b) roadway density.

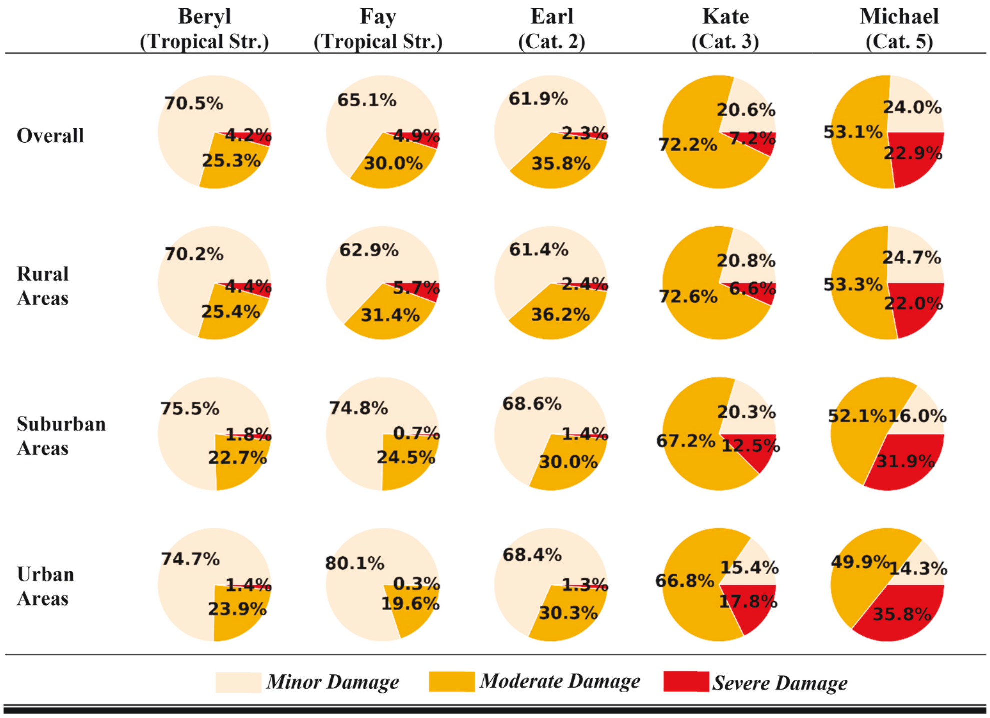

Fig. 4. Damage assessment based on population density.

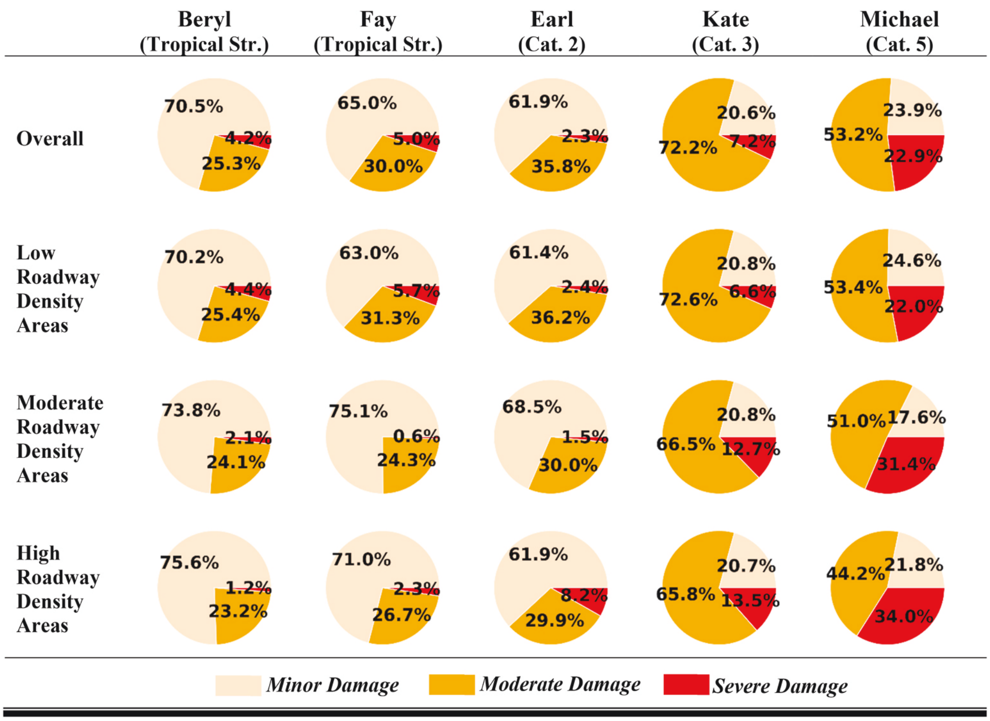

Fig. 5. Damage assessment based on roadway density.

population density. Much more severe damage was generated at moderate and high roadway density areas once the intensity of the hurricane reached higher levels with speeds of 120 mph. Low roadway density areas seemed to experience more moderate damage for all studied storms and hurricanes. Moderate roadway density areas, on the other hand, endured more minor damage for hurricane intensities associated with winds speeds less than 100 mph. The highest severe damage was caused by Hurricane Michael in high roadway density areas. This can be attributed to the fact that high roadway density areas are the main priority for debris removal operations and the remaining downed trees in the rural areas may result in high NDVI values in the aftermath of the hurricanes.

Suburban and urban areas, as well as moderate and high roadway density areas, are verified to suffer more severe damage when they experience high-intensity hurricanes. Among these, urban and high roadway density areas suffered more severe damage compared to suburban and moderate roadway density areas. Rural and low roadway density areas, on the contrary, faced more moderate damage than others in all types of hurricanes and storms. These findings are also proven by the average NDVI reduction per pixel (Fig. 6).

The average NDVI reduction per pixel are presented in Fig. 6a and b. Both indicate that Tropical Storm Beryl, Tropical Storm Fay, and Hurricane Earl caused NDVI reduction values less than 0.02 per pixel. The average NDVI reduction values of Hurricane Kate and Hurricane Michael were found as 0.09 and 0.11, respectively. The largest NDVI reduction per pixel was around 0.16, which occurred in urban areas and high roadway density areas.

4.2. USACE debris estimation

USACE hurricane debris estimating model was applied using the same data. The storm category multiplier (C) was based on the hurricane category. As aforementioned, the same multiplier was used for Tropical Strom Beryl and Fay as Hurricane Earl which is a Category 1 Hurricane. Vegetation multiplier (V) was determined by the initial NDVI before each hurricane occurred. Three equal intervals of initial NDVI were calculated from 0 to 1, and each interval is the range to determine the multiplier of vegetation factor. Commercial characteristics multiplier (B) was chosen as light with a 1.0 multiplier considering all shopping centers, industrial and manufacturing facilities within the Bay County area.

The outcomes of USACE debris estimation are plotted in Fig. 7a and Fig. 7b. Note that both figures are log-linear plots, where the debris volume is log-scale and maximum intensity is a linear scale. The results indicate that Tropical Storm Beryl, Tropical Storm Fay, and Hurricane Earl generated debris around log (1.1×10^9) cy while Hurricane Kate generated debris around log (1.6×10^{10}) cy and Hurricane Michael generates debris around log (6×10^{10}) cy. It is clear that debris caused by hurricanes and storms happened to be minimal as long as the intensity of the hurricane is low with wind speeds less than 100 mph.

Unlike the NDVI reduction, the debris increased by a factor of 14.5 when the wind speeds reached 120 mph. After this point, the debris increased by a factor of 3.7 with speeds of 160 mph. In the USACE method, it is apparent that the factors of population density and roadway density affected the debris estimation only to a small degree (less than 5% difference). This is a critical analytical finding that indicates the differences between the USACE method and the proposed NDVI reduction method regarding demographic factors.

Fig. 8a and Fig. 8b show the average estimated debris volume in each pixel. Tropical Storm Beryl, Tropical Storm Fay, and Hurricane Earl created debris less than 1000 cy per pixel whereas Hurricane Kate and Hurricane Michael caused debris around 5000 cy and 20,000 cy per pixel. Both figures indicate that suburban and moderate roadway density areas generated more debris than rural and low roadway density areas. Meanwhile, urban and high roadway density areas produced more debris than suburban and moderate roadway density areas. This pattern is identical to the findings of the NDVI reduction analysis despite the fact that USACE debris volume increases exponentially for the urban and suburban areas for very high intensity storms. This could be attributed from the fact that the debris volume estimation method is heavily weighted on the number of households and storm intensity variable “C”. Particularly, high-intensity hurricanes would enlarge this difference of average estimated debris at each pixel.

4.3. Damage evaluation comparison using USACE and NDVI reduction approaches

Using the observations of hurricane damage evaluations based on NDVI Reductions and USACE’s debris volume estimation, a new model was developed to estimate the volume of debris depending solely on the NDVI reduction. Fig. 9 presents the goodness-of-fit of the calculated debris from the USACE method and total NDVI reduction obtained from the proposed methodology. It can be observed that a practically exponential relationship is present based on the utilized log-linear plot. As observed in the graph, the function fits well as validated by the R-square value of 0.97. The function is presented in Equation [3] below.

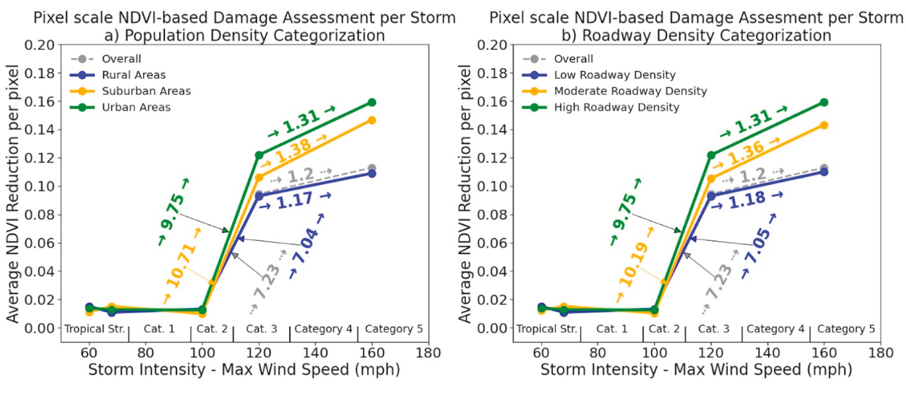

Fig. 6. Average NDVI reduction per pixel weighted on (a) population and (b) roadway.

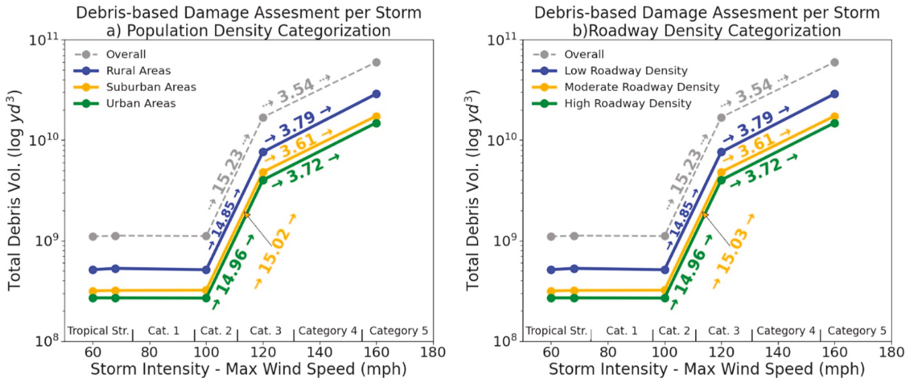

Fig. 7. USACE debris volume estimation based on (a) population and (b) roadway density.

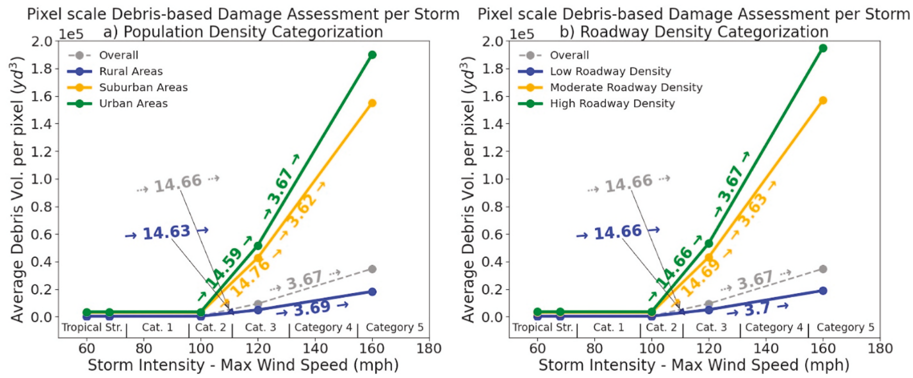

Fig. 8. Average debris per pixel based on (a) population and (b) roadway density.

$$Y = 700000000 * e^{0.00001 * x} \tag{3}$$

where x represents total NDVI reduction and Y represents debris in log (cy), which was estimated as the natural log of the USACE's debris volume estimation formula.

Note that the USACE Emergency Management staff has developed a debris estimation model based on actual data from Hurricanes Frederic, Hugo, and Andrew. Also, the major factors used by the model are the number of households, hurricane intensity, vegetative cover, commercial density, and precipitation. This model is acknowledged to have an error of nearly 30%. In addition, the USACE debris model's multiplier of vegetation input is extracted from the pre-storm NDVI values in this study, while the pre-storm NDVI is also used to determine the reduction of NDVI.

In our comparative assessment, the total NDVI reduction is found to have a strong and positive exponential relationship with debris estimated using the USACE method. The exponential relationship between the two methods indicates that the USACE debris model could be overestimating the debris caused for a hurricane that is Category 3 or greater especially in the urban and suburban areas. Particularly, a higher intensity hurricane would enlarge this error. For lower strength hurricanes, on the other hand, both the USACE model and the proposed approach provided similar results.

5. Conclusion and future work

There will be failed or disrupted segments on a transportation network after a hurricane as a function of rising water, downed trees/branches, and debris accumulation [39]. Hence, understanding hurricane damage in the context of debris and vegetation decrease is one of the key concerns for the transportation network recovery in the aftermath of a hurricane. Remote sensing-derived spectral indices are versatile and convenient tools to incorporate hurricane damage within this context. Therefore, in this paper, the impacts of different hurricanes and storms on coastal communities have been evaluated and compared using the data on NDVI reduction, and population and roadway densities. For this research, three hurricanes and two tropical storms with different strengths that hit Bay County, Florida were selected. NDVI values were derived from the NASA's Landsat satellites. Specifically, the amount of NDVI reduction from before and after landfall of each hurricane was quantified for the Bay County area. The variability of NDVI reduction of each hurricane was examined and compared with others. Additionally, the hidden variety on the damage was highlighted with categorized analyses focusing on the different population and roadway densities.

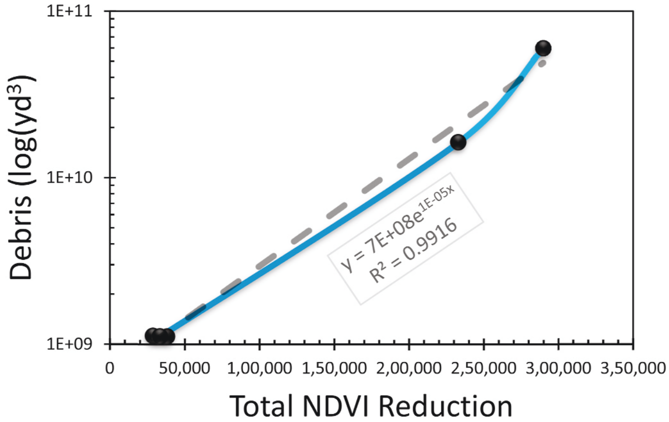

Fig. 9. Fitting NDVI Reduction-based debris estimation on the USACE's method.

The existing debris estimation model developed by USACE was also evaluated using the same dataset. Results from the model present similar patterns to the findings of the developed methodology based on the NDVI reduction. It was found that suburban areas, urban areas, moderate and high roadway density areas generated more debris and NDVI changes than rural and low roadway density areas. Particularly, high-intensity hurricanes would enlarge this difference. Such an implementation of remote sensing techniques that can measure the vegetative response to hurricanes can enable mapping the spatial patterns of hurricane impact on coastal communities. Understanding the changes of NDVI following a major hurricane may also lead to improved emergency management strategies.

Findings of this study can assist transportation and emergency professionals to conduct a damage assessment of hurricanes while benefiting the logistics of quickly coordinating and implementing an extensive remote sensing-based damage survey. Additionally, the results can help predictive understanding of the long-term effects of hurricanes on coastal communities and eventually develop quantitative models to explain the relationships between the storm intensity and the resulting severity of damage on the different zones of the impacted areas. Moreover, this study puts a spotlight on how urbanization and critical infrastructure may affect the extent of the damage caused by hurricanes, which may help communities and emergency professionals determine prioritizing areas during the pre-storm preparedness.

This study inevitably has its own limitations, and there are possible future work directions. Although NDVI has been widely used in ecological research and it has been found to be a robust and reliable indicator, NDVI carries only a fraction of the information available in the original spectral reflectance data and can be affected by factors such as atmosphere, clouds, soil, and sun angle. Also, NDVI tends to estimate a large number of vegetation properties, which is not perfect for an urban environment. A future study can modify NDVI or develop new indices to estimate the hurricane damage. Moreover, this study is lacking Category 2 and 4 hurricanes for intensity assessment due to the unavailability of data for the study area. Future research can be conducted using all types of the intensity of hurricanes and multiple study areas. The demographic factors other than population and roadway networks can also be utilized, including age, household, income, commercialization, and power networks.

Author contributions

The authors confirm contribution to the paper as follows: study conception and design: A. Karaer, M. Chen, T. Abichou, and E. Ozguven data collection: A. Karaer and M. Chen analysis and interpretation of results: A. Karaer, M. Chen, M. Gazzea, M. Ghorbanzadeh, T. Abichou, R. Arghandeh and E. Ozguven draft manuscript preparation: A. Karaer, M. Chen, M. Gazzea, M. Ghorbanzadeh, T. Abichou, R. Arghandeh and E. Ozguven. All authors reviewed the results and approved the final version of the manuscript.

Declaration of competing interest

The authors declare that they have no known competing financial interests or personal relationships that could have appeared to influence the work reported in this paper.

References

[1] C.J. Friedman, Residential Building Damage from Hurricane Storm Surge: Proposed Methodologies to Describe, Assess and Model Building Damage, 2009.
[2] C. Massarra, Hurricane Damage Assessment Process for Residential Buildings, 2012.
[3] A. Karaer, M.B. Ulak, T. Abichou, R. Arghandeh, E.E. Ozguven, Post-hurricane vegetative debris assessment using spectral indices derived from satellite imagery, Transport. Res. Rec.: J. Transport. Res. Board (2021), https://doi.org/10.1177/03611981211029921, 036119812110299.
[4] M. Ghorbanzadeh, M. Koloushani, E.E. Ozguven, A. Vanli, R. Arghandeh, City Transportation Network Vulnerability to Disasters: the Case of Hurricane Hermine in Florida, Environmental Hazards, 2021, pp. 1–19, https://doi.org/10.1080/17477891.2021.1933885.
[5] M.B. Ulak, A. Kocatepe, L.M. Konila Sriram, E.E. Ozguven, R. Arghandeh, Assessment of the hurricane-induced power outages from a demographic, socioeconomic, and transportation perspective, Nat. Hazards 92 (No. 3) (2018) 1489–1508, https://doi.org/10.1007/s11069-018-3260-9.
[6] A. Kocatepe, M.B. Ulak, G. Kakareko, E.E. Ozguven, S. Jung, R. Arghandeh, Measuring the accessibility of critical facilities in the presence of hurricane-related roadway closures and an approach for predicting future roadway disruptions, Nat. Hazards 95 (No. 3) (2019) 615–635, https://doi.org/10.1007/s11069-018-3507-5.

[7] M. Gazzea, A. Karaer, M. Ghorbanzadeh, N. Balafkan, T. Abichou, E.E. Ozguven, R. Arghandeh, Automated satellite-based assessment of hurricane impacts on roadways, IEEE Trans. Ind. Inf. (2021), https://doi.org/10.1109/TII.2021.3082906.
[8] C. Houser, Geomorphological controls on road damage during hurricanes Ivan and Dennis, J. Coast Res. 253 (2009) 558–568, https://doi.org/10.2112/07-0923.1.
[9] M. Ghorbanzadeh, M. Koloushani, M.B. Ulak, E.E. Ozguven, R.A. Jouneghani, Statistical and spatial analysis of hurricane-induced roadway closures and power outages, Energies 13 (No. 5) (2020) 1098, https://doi.org/10.3390/en13051098.
[10] M.A.A. Hoque, S. Phinn, C. Roelfsema, I. Childs, Tropical cyclone disaster management using remote sensing and spatial analysis: a review, Int. J. Disaster Risk Reduc. 22 (No. September 2016) (2017) 345–354, https://doi.org/10.1016/j.ijdrr.2017.02.008.
[11] M. Chen, A. Karaer, E.E. Ozguven, T. Abichou, R. Arghandeh, J. Nienhius, Developing city-wide hurricane impact maps using real-life data on infrastructure, vegetation and weather, Transport. Res. Rec.: J. Transport. Res. Board 2675 (No. 3) (2021) 393–404, https://doi.org/10.1177/0361198120972714.
[12] S. Jiang, C.J. Friedland, Automatic urban debris zone extraction from post-hurricane very high-resolution satellite and aerial imagery, Geomatics, Nat. Hazards Risk 7 (No. 3) (2016) 933–952, https://doi.org/10.1080/19475705.2014.1003417.
[13] W. Wang, J.J. Qu, X. Hao, Y. Liu, J.A. Stanturf, Post-hurricane forest damage assessment using satellite remote sensing, Agric. For. Meteorol. 150 (No. 1) (2010) 122–132, https://doi.org/10.1016/j.agrformet.2009.09.009.
[14] P. Drenan, S. Treloar, A Debris Management Handbook for State and Local DOTs and Departments of Public Works, Transportation Research Board, 2014.
[15] FEMA, Public Assistance Debris Management Guide, 2007.
[16] NOAA, *Hurricanes and Tropical Storms - Annu*al 2018, 2019.
[17] U.S. Census Bureau. QuickFacts: Bay County, Florida. https://www.census.gov/quickfacts/fact/table/baycountyflorida#. Accessed Aug. 1, 2021.
[18] Max Mayfield, Preliminary Reprot Tropical Storm Beryl, 1994.
[19] S.R. Stewart, J.L. Beven, Tropical Cyclone Report-Tropcial Storm Fay (2008), 2009.
[20] S. Ma, H. Ritchie, J. Gyakum, J. Abraham, C. Fogarty, R. McTaggart-Cowan, A study of the extratropical reintensification of former hurricane Earl using Canadian meteorological centre regional analyses and ensemble forecasts, Mon. Weather Rev. 131 (No. 7) (2003) 1342–1359, https://doi.org/10.1175/1520-0493(2003)131<1342:ASOTER>2.0.CO;2.
[21] E.S. Blake, E.N. Rappaport, The Deadliest, Costliest, and Most Intense United States Tropical Cyclones from 1851 to 2006 (And Other Frequently Requested Hurricane Facts), 2001.
[22] National Oceanic and Atmospheric Administration, Hurricane Michael 2018, 2018.
[23] ESRI. ArcGIS Living Atlas of the World. https://livingatlas.arcgis.com/en/home/. Accessed Jul. 26, 2021.
[24] T. Schott, C. Landsea, G. Hafele, J. Lorens, H. Thurm, B. Ward, M. Willis, W. Zaleski, The Saffir-Simpson Hurricane Wind Scale, National Hurricane Center, No. February, 2012, pp. 1–4.
[25] NASA, Landsat timeline. https://landsat.gsfc.nasa.gov/about/landsat-timeline/. (Accessed 13 February 2022). Accessed.
[26] Google Earth Engine, Landsat 5 TM collection NDVI composite. https://developers.google.com/earth-engine/datasets/catalog/LANDSAT_LT05_C01_T1_32DAY_NDVI. (Accessed 13 February 2022). Accessed.
[27] Z. Zhu, C.E. Woodcock, Object-based cloud and cloud shadow detection in Landsat imagery, Remote Sens. Environ. 118 (2012) 83–94, https://doi.org/10.1016/j.rse.2011.10.028.
[28] T. Hu, R.B. Smith, The impact of hurricane maria on the vegetation of Dominica and Puerto Rico using multispectral remote sensing, Rem. Sens. 10 (No. 6) (2018), https://doi.org/10.3390/rs10060827.
[29] United States Census Bureau. American Community Survey (ACS). https://www.census.gov/acs/www/data/data-tables-and-tools/data-profiles/. Accessed Jul. 31, 2020.
[30] U.S. Census Bureau. TIGER Line Data Set. https://www.census.gov/cgi-bin/geo/shapefiles/index.php. Accessed Jun. 9, 2020.
[31] MapBox. Rasterio: Access to Geospatial Raster Data. https://rasterio.readthedocs.io/en/latest/. Accessed Feb. 13, 2022.
[32] USACE. *Debris Management Guide, APPENDIX A: Hurricane Debris Estimation Model*, Washington D.C., 2008.
[33] B.K. Thompson, F.J. Escobedo, C.L. Staudhammer, C.J. Matyas, Y. Qiu, Modeling hurricane-caused urban forest debris in Houston, Texas, Landsc. Urban Plann. 101 (No. 3) (2011) 286–297, https://doi.org/10.1016/j.landurbplan.2011.02.034.
[34] F.J. Escobedo, C.J. Luley, J. Bond, C. Staudhammer, C. Bartel, Hurricane debris and damage assessment for Florida urban forests, Arboric. Urban For. 35 (No. 2) (2009) 100–106.
[35] B. Thompson, F.J. Escobedo, C.L. Staudhammer, J. Bond, C. Luley, Urban Forests in Florida: Storm Damage Assessment Utility for Estimating Hurricane-Caused Tree Debris, Publication FOR268, 2010.
[36] C.L. Staudhammer, F. Escobedo, C. Luley, J. Bond, Patterns of urban forest debris from the 2004 and 2005 Florida hurricane seasons, South. J. Appl. For. 33 (No. 4) (2009) 193–196, https://doi.org/10.1093/sjaf/33.4.193.
[37] M.L. Duryea, E. Kampf, R.C. Littell, C.D. Rodríguez-Pedraza, Hurricanes and the urban forest: I. Effects on southeastern United States coastal plain tree species, Arboric. Urban For. 33 (No. 2) (2007) 98–112.
[38] M.L. Duryea, E. Kampf, R.C. Littell, C.D. Rodríguez-Pedraza, Hurricanes and the urban forest: II. Effects on tropical and subtropical tree species, Arboric. Urban For. 33 (No. 2) (2007) 98–112.
[39] M.W. Horner, M.J. Widener, The effects of transportation network failure on people's accessibility to hurricane disaster relief goods: a modeling approach and application to a Florida case study, Nat. Hazards 59 (No. 3) (2011) 1619–1634, https://doi.org/10.1007/s11069-011-9855-z.
[40] A. Karaer, M.B. Ulak, T. Abichou, R. Arghandeh, E.E. Ozguven, Leveraging Remote Sensing Indices for Hurricane-Induced Vegetative Debris Assessment: A GIS-Based Case Study for Hurricane Michael, in: Presented at 100th Annual Meeting of the Transportation Research Board, Washington, D.C., 2021. No. TRBAM-21-04450.
[41] A. Karaer, M.B. Ulak, T. Abichou, R. Arghandeh, E.E. Ozguven, Leveraging Remote Sensing Indices for Hurricane-Induced Vegetative Debris Assessment: A GIS-Based Case Study for Hurricane Michael, in: Presented at 100th Annual Meeting of the Transportation Research Board, Washington, D.C., 2021. No. TRBAM-21-04450.
[42] A Karaer, MB Ulak, EE Ozguven, T Sando, Reducing the Non-Recurrent Freeway Congestion with Detour Operations: Case Study in Florida, Transportation Engineering 2 (2020) 100026.
[43] A Karaer, N Balafkan, M Gazzea, R Arghandeh, EE Ozguven, Analyzing COVID-19 impacts on vehicle travels and daily nitrogen dioxide (NO2) levels among Florida counties, Energies 13 (22) (2020) 6044.